Journal of
Ceramic Science
and Technology

J. Ceram. Sci. Tech., **04** [03] 151-156 (2013)
DOI: 10.4416/JCST2013-00005
available online at: http://www.ceramic-science.com

Phase Transformation of $10Li_2O$-$9MnO_2$-$16Fe_2O_3$-$15CaO$-$5P_2O_5$-$5Al_2O_3$-$40SiO_2$ Glass

H.-Z. Cheng[1], H.-J. Lin[2], C.-S. Hsi*[2], C.-F. Wang[1], M.-C. Wang*[3], H. Jiang[4], C.-J. Li[4], P. Lu[5, 6]

[1]Department of Materials Science and Engineering, I-Shou University, 1 Huseh-Cheng Road, Section 1, Ta-Hsu, Kaohsiung 84001, Taiwan
[2]Department of Materials Science and Engineering, National United University, 1 Lien-Da Road, Kung-Ching Li, Miao-Li 36003, Taiwan
[3]Department of Fragrance and Cosmetic Science, Kaohsiung Medical University, 100 Shih-Chuan 1st Road, Kaohsiung 80708, Taiwan
[4]Special Glass Key Laboratory of Hainan Province, Hainan University, 58 People Road, Haikou City, Hainan Province, P.R. China
[5]Aviation Industry Corporation of China (Hainan) Special Glass Materials Co., LTD. South First Road, Economic Development Zone of Old City, Hainan Province, P.R. China
[6]Special Glass Engineering Technology Research Center of Hainan Province

received March 16, 2013; received in revised form May 5, 2013; accepted June 5, 2013

Abstract

The phase transformation and magnetic properties of $10Li_2O$-$9MnO_2$-$16Fe_2O_3$-$15CaO$-$5P_2O_5$-$5Al_2O_3$-$40SiO_2$ (LMFCPAS) glass have been observed and investigated using x-ray diffraction (XRD), scanning electron microscopy (SEM), energy-dispersive x-ray spectrometry (EDS), and transmission electron microscopy (TEM) with selected area electron diffraction (SAED). After crystallization of the LMFCPAS glass at 800 °C for 2 h, the crystalline phases of $Li_2Al_2Si_3O_{10}$, Li_2SiO_3, β-wollastonite (β-$CaSiO_3$), lithium orthophosphate (Li_3PO_4), magnetite ($FeFe_2O_4$) and triphytite ($Li(Mn_{0.5}Fe_{0.5})PO_4$) were obtained. When the LMFCPAS glass crystallized at 850 °C, the β-wollastonite exhibited lath form morphology. As the LMFCPAS glass crystallized at 850 °C for 16 h and under an applied magnetic field of 1000 Oe, very small remnant magnetic induction and coercive force of 0.01 emu/g and 50 Oe were obtained, respectively.

Keywords: LMFCPAS glass, crystallization behavior, lath form

I. Introduction

The developments of ferromagnetic glass-ceramics such as CaO-SiO_2-P_2O_3-Fe_2O_3 [1], CaO-SiO_2-P_2O_5-Na_2O-Fe_2O_3 [2, 3], Li_2O-Al_2O_3-SiO_2-Fe_2O_3-P_2O_5 [4] and CaO-SiO_2-(Fe, Fe_2O_3) [5] glasses by means of well-controlled crystallization processing have been reported previously. Some other studies attempted to change the matrix glass compositions by partially replacing oxides with MgO and ZnO [9, 10], or BaO and B_2O_3 [11, 12]. In 2011, Ferreira da Silva and Costa [9] demonstrated that the amount and type of preferential nanocrystalline zinc ferrite in Fe_2O_3-ZnO-MgO-SiO_2 crystallized glasses were affected by the glass compositions and heat treatment temperature. Mirkazemi *et al.* [11] also reported that the crystalline phases of BaB_2O_4 and $BaFe_{12}O_{19}$ appeared when $45BaO$-$25Fe_2O_3$-$30B_2O_3$ glasses powders were crystallized at 702 °C for 1 h. Their report also pointed out that BaB_2O_4 appeared first and subsequently the $BaFe_{12}O_{19}$ particles formed within the $Ba_2B_2O_4$-rich regions, which serve as suitably heterogeneous nucleation sites for their formation.

The crystallization kinetics of the Li_2O-MnO_2-Fe_2O_3-CaO-P_2O_5-SiO_2 glass systems using a non-isothermal method have been studied by Hsi *et al.* [6,7]. In addition, the crystallization kinetics and magnetic properties of iron oxide addition to $25Li_2O$-$8MnO_2$-$20CaO$-$2P_2O_5$-$45SiO_2$ glasses have also reported by Hsi *et al.* [8]. The phase of (Li, Mn) ferrite was also reported to appear in this glass system after crystallization treatment. To avoid the appearance of (Li, Mn) ferrite in the Li_2O-MnO_2-Fe_2O_3-CaO-P_2O_5-SiO_2 glass systems, the Li_2O content in the glass composition needs to be reduced, but the Fe_2O_3 content and the addition of Al_2O_3 need to be increased in the glass composition, which eventually formed the $10Li_2O$-$9MnO_2$-$16Fe_2O_3$-$15CaO$-$5P_2O_5$-$5Al_2O_3$-$40SiO_2$ glass (hereafter abbreviated to LMFCPAS glass).

This paper intends to report on the phase transformation and magnetic properties of the LMFCPAS glass, which has been studied in detail. X-ray diffraction (XRD), scanning electron microscopy (SEM), energy-dispersive x-ray

* Corresponding author: chsi@nuu.edu.tw (C.S. Hsi)
mcwang@kmu.edu.tw (M.C. Wang)

spectrometry (EDS), transmission electron microscopy (TEM), selected area electron diffraction (SAED) were applied to investigate the phase transformation of LMFCPAS glass. In addition, a superconducting quantum interference device (SQID) was used for measuring the magnetic properties of crystallized LMFCPAS glass. The purpose of this investigation was first to study the phase transformation of LMFCPAS glass, second to examine the microstructure of crystallized LMFCPAS glass and finally to evaluate the magnetic properties of crystallized LMFCPAS glass.

II. Experimental Procedure

(1) Sample preparation

The reagent grade powders of Li_2CO_3, MnO_2, $CaHPO_4{\cdot}2H_2O$, $CaCO_3$, Al_2O_3, and SiO_2 with purity higher than 98 % supplied by Nihon Shiyak Industries, LTD., Osaka, Japan, and Fe_2O_3 supplied by Kanto Chemical Co., Inc., Tokyo, Japan were used for preparing LMFCPAS glass. The weight percentage of Li_2O, MnO_2, Fe_2O_3, CaO, P_2O_5, Al_2O_3, and SiO_2 in the glass was 10.0 %, 9.0 % 16.0 %, 15.0 % 5.0 %, 5.0 % and 40.0 %, respectively. All samples obtained in 50 to 100 g batches with specified composition were accurately weighed and thoroughly premixed. The batches were transferred to a mullite crucible and melted at 1450 °C in an electric furnace for 2 h. After that, the melt was quenched in water, dried and crushed. To obtain a homogeneous composition of LMFCPAS glass, the crushed powders were re-melted at 1450 °C for 2 h. The glass melt was then cast onto a stainless steel plate at 400 °C, subsequently transferred to an annealing furnace and held at 400 °C for 2 – 4 h, and cooled down in the furnace to the room temperature at a rate of 10 °C/min. Finally, a piece of dark colored glass was obtained.

After it had been annealed, the LMFCPAS glass was cut into the lath shape with the length and width of 5 cm and 1.5 cm, respectively. The lath samples were crystallized at various temperatures for different durations, and then the LMFCPAS glass ceramics were obtained.

(2) Sample characterization

The crystalline phases of LMFCPAS glass-ceramics were identified with an x-ray diffractometer (XRD, D-MAX III B, Riguku, Japan) with Cu Kα radiation and a Ni filter. The operating voltage and current were 30 kV and 20 mA, respectively, at a scanning rate (2θ) of 0.25°/min from 10 to 60°. A scanning electron microscope (SEM, Hitachi S-2700, Japan) was used to observe the crystallized samples. Chemical microanalysis was conducted with an energy-dispersive x-ray spectrometer (EDS, Noran 432 C, USA). All samples prepared for SEM observation were polished, etched with diluted acid solution (5 parts HF, 2 parts HCl and 93 parts distilled water) and coated with a thin layer of a conductive film. Thin foils for a transmission electron microscope (TEM, Hitachi HF-2000, Tokyo, Japan) were prepared with the conventional technique: the sample was sliced to a thickness of about 200 μm with a diamond-embedded saw, and then lapped mechanically to a thickness of about 30 μm and ion-beam thinned to electron transparency. The TEM accelerating voltage was 200 kV. Selected area electron diffraction (SAED) examinations were performed on carefully thinned foils of the crystallized samples.

Magnetic measurements were conducted using a superconducting quantum interference device (SQUID) magnetometer with the applied field up to 6 T.

III. Results and Discussion

(1) Crystallization behavior of the LMFCPAS glass

The effect of the crystallization temperature on the progressive development of phase transformation was studied based on the XRD patterns of the LMFCPAS glass crystallized at various temperatures for 2 h as shown in Fig. 1. It is found that (a) the glassy state was still maintained up to 700 °C as shown in Fig. 1(a). In comparison with the JCPDS database, the lithium aluminosilicate ($Li_2Al_2Si_3O_{10}$) (JCPDS Card No.25 – 1180), β-wollastonite (β-$CaSiO_3$) (JCPDS Card No.42 – 547) and lithium orthophosphate (Li_3PO_4) (JCPDS Card No.84 – 0046) phases appeared in the LMFCPAS glass specimen crystallized at 750 °C as shown in Fig. 1(b). It is worth noting that diffraction peaks of the magnetite ($FeFe_2O_4$) (JCPDS Card No.19 – 627) also appear in this XRD pattern but the intensity is still weak. The XRD pattern of LMFCPAS glass crystallized at 800 °C as shown in Fig. 1 (c) reveals the appearance of lithium silicate phase (Li_2SiO_3) (JCPDS Card No.29 – 829). The notably sharp diffraction peaks shown in Fig. 1 (c) indicate that there are $Li_2Al_2Si_3O_{10}$, β-wollastonite, Li_3PO_4 and $FeFe_2O_4$ phases. In addition, a minor crystalline phase of triphylite [$Li(Mn_{0.5}Fe_{0.5})PO_4$] (JCPDS Card No.11 – 456) also shows up. Fig. 1 (d) shows that the phases obtained in the specimen crystallized at 850 °C are similar to those crystallized at 800 °C.

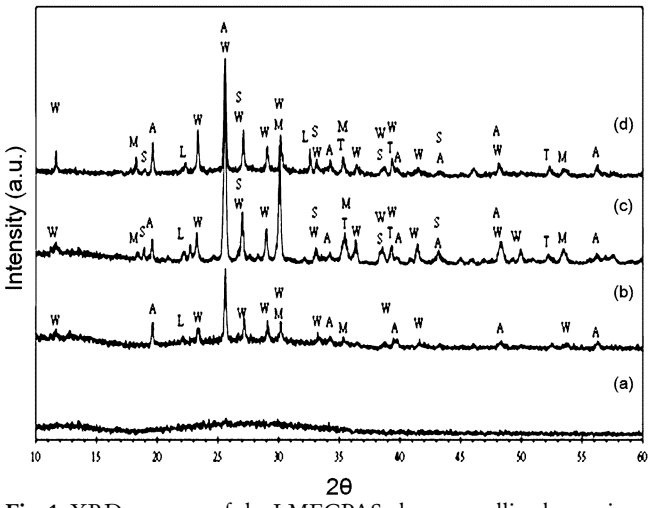

Fig. 1: XRD patterns of the LMFCPAS glass crystallized at various temperatures for 2 h: (a) 700 °C, (b) 750 °C, (c) 800 °C and (d) 850 °C, S: lithium silicate (Li_2SiO_3), W: β-wollastonite (β-$CaSiO_3$), M: magnetite ($FeFe_2O_4$), L: lithium orthophosphate (Li_3PO_4), T: triphytite ($Li(Mn_{0.5}Fe_{0.5})PO_4$), A: $Li_2Al_2Si_3O_{18}$.

The iron oxide contained $25Li_2O$-$8MnO_2$-$20CaO$-$2P_2O_5$-$45SiO_2$ glass (LMCPS, $0 \le Fe_2O_3 \le 8$ at% extra addition) was heat-treated at various temperatures for 4 h to demonstrate the phase development of magnetic glass-

ceramics by Hsi *et al.* [8]. They pointed out that when the LMCPS glass without the addition of Fe_2O_3 was heat-treated at 720 °C, the glass-ceramic contained $LiMn_2O_4$, β-$CaSiO_3$, $Li_2Ca_4Si_4O_{13}$ and $Ca(Ca, Mn)Si_2O_6$ phases. However, the (Li, Mn) ferrite gradually formed and became the minor phase for the LMCPS glass crystallized at 720 °C with extra addition of 4 at% and 8 at% Fe_2O_3. With the addition of extra Fe_2O_3, it was also shown that the $LiMn_2O_4$ became the minor phase for crystallization at 850 °C but the rest of crystalline phases shown in this LMCPS glass sample were the same as those crystallized at 720 °C without the addition of Fe_2O_3. It was clear that as the amount of Fe_2O_3 addition increased, the (Li, Mn) ferrite became more evident but the $LiMn_2O_4$ phase gradually decreased and finally started to form the $Li_2FeMn_3O_8$ phase as the amount of Fe_2O_3 added reached 8 at% [8].

In a comparison of the phase transformation behavior of the present results with the previous study [8], it was found that crystalline phases observed in two studies are quite different except the β-wollastonite. The main reason for such discrepancy is that compositions for these two glass systems are quite different. The glass composition of previous study [8] contained 25 at% Li_2O; the high content of Li_2O might benefit the decrease in viscosity of the glass and the formation of Li_2MnO_4 at 600 °C. However, there was only 10 wt% Li_2O in the glass system of this study; the sample could still maintain the amorphous state for LMFCPAS glass crystallized at 700 °C for 2 h. Furthermore, the magnetite, triphylite and lithium aluminosilicate phases were shown in the present study, but not the (Li, Mn) ferrite.

In addition, the $4.5MgO$-$(45\text{-}x)CaO$-$34SiO_2$-$16P_2O_5$-$0.5CaF$-xFe_2O_3 ($5\ wt\% \le x \le 20\ wt\%$) glass crystallized at 1050 °C for 3 h have been closely studied by Singh and Srinivasan [13]. They pointed out that the crystalline phases of hydroxyapatite, wollastonite and magnetic appeared in all glass-ceramic samples. The additional phase of akermanite ($Ca_2MgSi_2O_7$) was developed in the glass-ceramics samples when the glass composition of Fe_2O_3 was greater than 10 wt%. Singh *et al.* [3] also pointed out that the hydroxyapatite ($Ca_{10}(PO_4)_6(OH)_2$), magnetite and wollastonite were the major phases in $41CaO$-$(52\text{-}x)SiO_2$-$4P_2O_5$-xFe_2O_3-$3Na_2O$ ($2 \le x \le 10$ mol%) glasses heat-treated at 1050 °C for 3 h. In a comparison with the results from present work and that of the Singh *et al.* [3], it is found that most of the crystalline phases that appeared in these two recrystallized glass systems are different except the magnetic and wollastonite phases [3, 13]. The different crystalline phases in two glass systems are apparently caused by the different composition and crystallized temperature.

(2) Microstructure of the LMFCPAS glass-ceramics

The SEM microstructure of the LMFCPAS glass crystallized at 850 °C for various times is shown in Fig. 2. Fig. 2(a) shows the morphology of the LMFCPAS glass crystallized at 850 °C for 2 h. As indicated by arrows, there are three distinct regions, the dispersed particles region, light-gray region and deep-gray region in this SEM micrograph. The light-gray and deep-gray are presented in narrow strip form. EDS results from three regions in Fig. 2(a) reveal that the deep-gray region primarily contained the ratio of Si 56.30 wt%, Al 26.63 wt%, Ca 5.32 wt% and O 17.45 wt%, whereas the light-gray region primarily contained the ratio of Si 52.50 wt%, Ca 35.00 wt%, O 9.50 wt% and Mn 3.00 wt%. Integrating the results of XRD and EDS, the deep-gray region ((Al,Si)-rich) is identified as the $Li_2Al_2Si_3O_{10}$ phase and the light-gray region as the β-$CaSiO_3$ phase. Moreover, both β-$CaSiO_3$ and $Li_2Al_2Si_3O_{10}$ show obviously directional growth. Fig. 2(a) also shows the β-$CaSiO_3$ phase is dominant and the lath structure of β-$CaSiO_3$ breaks and becomes short as the crystallization time increases, as shown in Figs. 2(b) and (c). The $Li_2Al_2Si_3O_{10}$ phase also appears in a lath structure and is in close contact with the β-$CaSiO_3$.

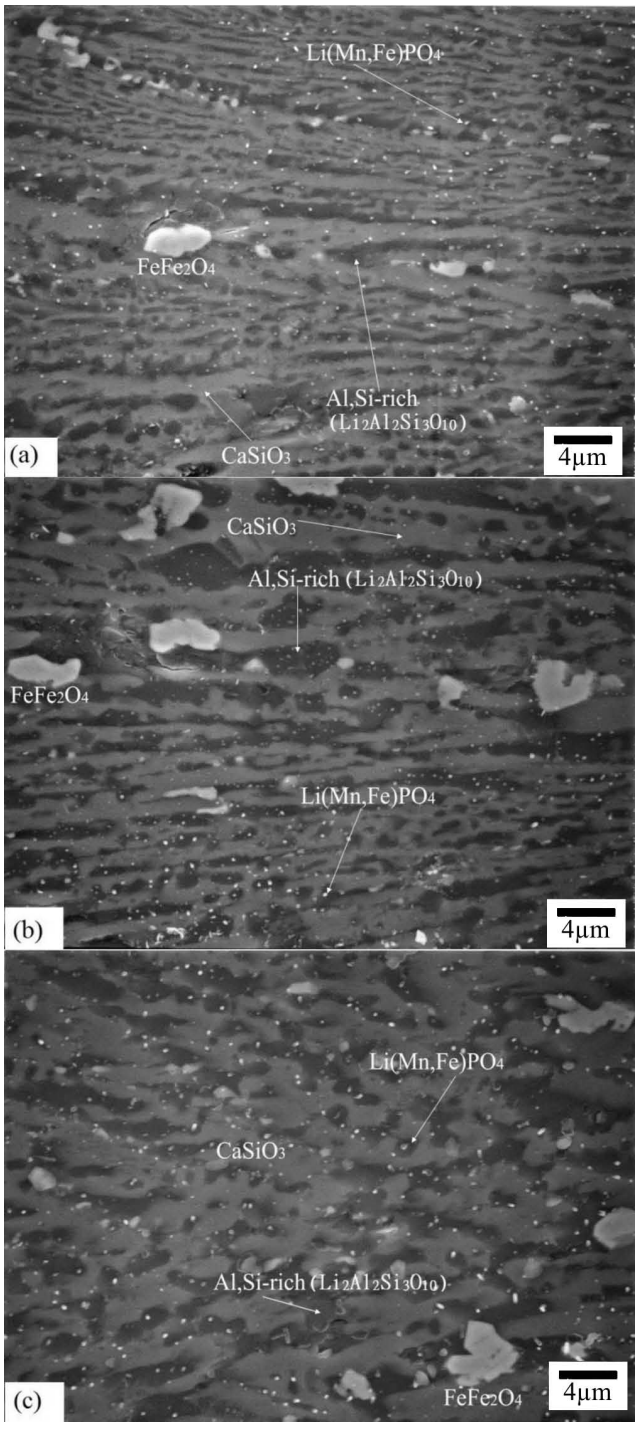

Fig. 2: SEM microstructure of the LMFCPAS glass crystallized at 850 °C for various lengths of time: (a) 2 h, (b) 8 h, and (c) 16 h.

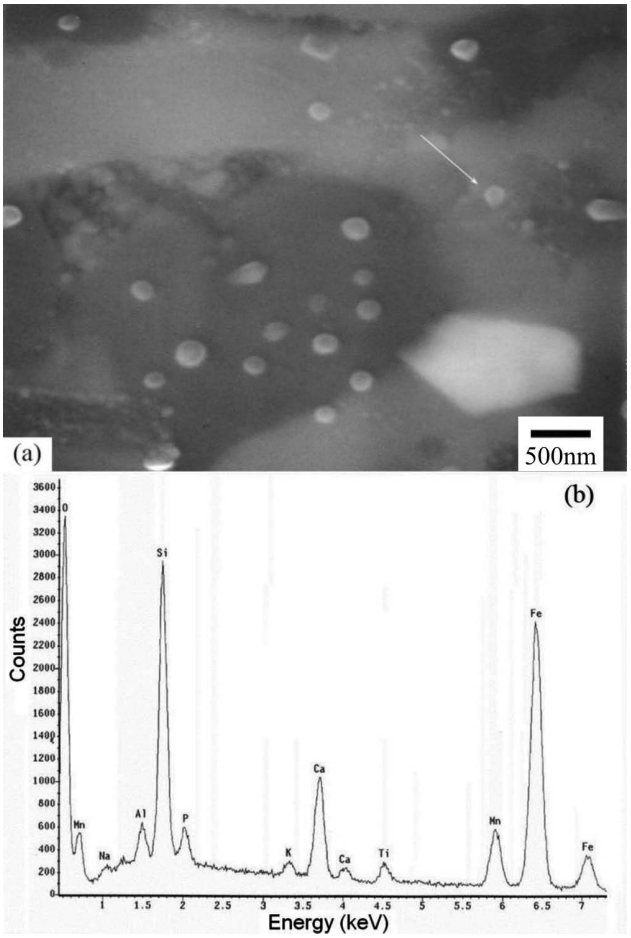

Fig. 3: Enlarged view of small particles in Fig. 2(a) and EDS result.

The SEM microstructure of the $35BaO\text{-}35Fe_2O_3\text{-}20B_2O_3\text{-}10SiO_2\text{-}1ZrO_2$ (added extra, as a nucleant) (by mol%) glass with one-step heat treatment at 720 °C for 1 h has been observed by Mirkazemi *et al.* [4]. They revealed that the $BaFe_{12}O_{19}$ phase in the crystallized glass sample appeared in diverse crystal shapes and sizes such as small particles, very fine needle-like or platelets with bigger size. Some large sizes of $BaFe_{12}O_{19}$ with a regular hexagonal shape were also found.

Also based on the one-step crystallization process, both morphologies of β-$CaSiO_3$ and $Li_2Al_2Si_3O_{10}$ are found to, be different from the droplet shape of the $BaFe_{12}O_{19}$. In addition, the dendritic structure was also reported in previous results [6], but not found in the present study.

Fig. 3 shows the enlarged view of SEM microstructure and EDS result of the LMFCPAS glass crystallized at 850 °C for 16 h. It can be seen that the small particle (as indicated by the arrow) is composed primarily of Mn, Fe, P and O elements. These small particles are identified as the $Li(Mn,Fe)PO_4$ phase.

Fig. 4 shows the TEM bright field (BF) micrograph and selected area electron diffraction (SAED) patterns of the LMFCPAS glass crystallized at 850 °C for 16 h. Fig. 4(a), the bright field (BF) image, shows the lath and plate structure. Fig. 4(b) is the SAED pattern of the black area on the upper right in Fig. 4(a), the index of which corresponds to $FeFe_2O_4$ with zone axis of $[1\,\bar{1}\,\bar{4}]$. Fig. 4(c) shows the SAED pattern of lath form morphology on the right in Fig. 4(a), the index of which corresponds to β-$CaSiO_3$ with a zone axis of [110].

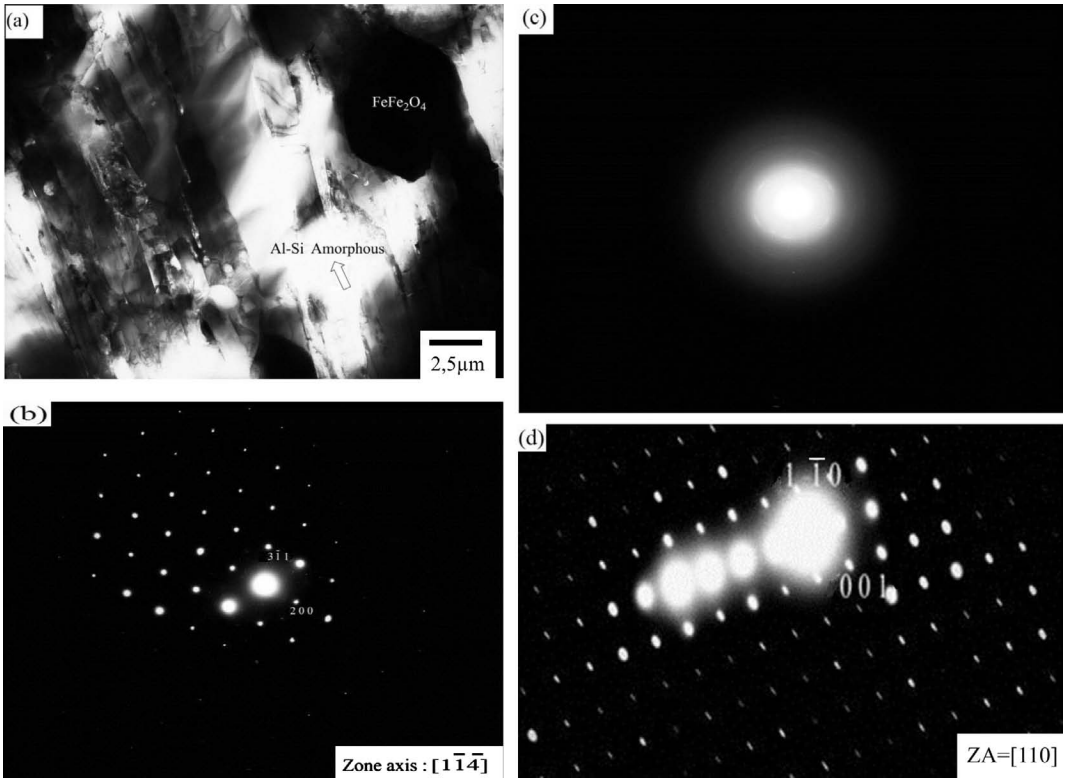

Fig. 4: TEM BF micrograph and SAED patterns of a specimen of LMFCPAS glass crystallized at 850 °C for 16 h: (a) BF image, (b) SAED pattern of the lath form structure on the upper right in Fig. 4(a), index corresponding to $FeFe_2O_4$ with zone axis $[1\,\bar{1}\,\bar{4}]$, (c) SAED pattern of the lath form structure on the right in Fig. 4(a), index corresponding to β-$CaSiO_3$ with zone axis of 110, and (d) SAED pattern index corresponding to Al-Si amorphous.

Fig. 4(d) is the SAED pattern of the white area denoted by the arrow in Fig. 4(a), the index of which corresponds to Al-Si amorphous.

(3) Magnetic properties of the LMFCPAS glass-ceramics

Fig. 5 shows the magnetization curve of the LMFCPAS glass crystallized at 850 °C for 16 h under a magnetic field of 1000 Oe. A very small remnant of magnetic induction and coercive force of 0.01 emu/g and 16 Oe were obtained, respectively. This result showed the ferromagnetic behavior of an inverse spinal structure.

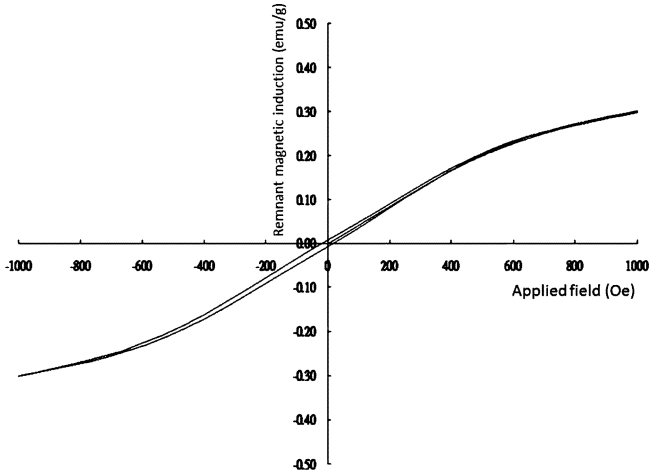

Fig. 5: Magnetization curve of the LMFCPAS glass crystallized at 850 °C for 16 h with the application of a magnetic field of 1000 Oe.

The remnant magnetization and coercive force of 0.71 emu/g and 91 Oe were obtained, respectively, when the $41CaO$-$42SiO_2$-$4P_2O_5$-$10Fe_2O_3$-$3Na_2O$ glass crystallized at 1050 °C for 3 h as reported by Singh *et al.* [3]. On the other hand, the coercive force and remnant magnetization were 63 Oe and lower than 0.5 emu/g, respectively, for the $25Li_2O$-$8MnO_2$-$20CaO$-$2P_2O_5$-$45SiO_2$-$8Fe_2O_3$ (added extra) (by mol%) glass crystallized at 850 °C for 4 h under an applied magnetic field of 300 Oe [8].

Chikazumi *et al.* [15] reported that a single domain structure in crystalline magnetic phase(s) was formed when the ferrite particles size is in the order of 10 – 50 nm for moderate crystal anisotropy. In addition, the coercive force was affected significantly by the amount and size of the magnetic crystallites in the crystallized glass samples reported by Singh and Srinivasan [13]. Comparing the result of present study and results of Hsi *et al.* [8], it is found that the size of magnetic phases in two studies was in the range of 2 – 3 μm, but the coercive force in the present study is 16 Oe, which is lower than that of 63 Oe in the previous study owing to the appearance of (Li, Mn) ferrite [8]. Furthermore, the coercive force and remnant magnetization of the present study were lower than that in the results reported by Singh *et al.* [3], which could be attributed to the average of magnetic phase of 26 nm only [3].

The specific absorption rate (SAR) value of heat generation depended on the coercive force and Fe_2O_3 content [16]. The coercive force of the $25Li_2O$-$8MnO_2$-$20CaO$-$2P_2O_5$-$45SiO_2$ (by at%) glass with extra addition of 8 at% and 16 at% Fe_2O_3 (denoted by F_3 and F_4) crystallized at 850 °C for 4 h was 63 and 100 Oe, respectively and the SAR value was 42.8 and 73.5 W/g, respectively. Although the value of SAR was not measured in the present study, the SAR value of the present study could be suggested to be lower than 42.8 W/g based on the low coercive force of 16 Oe compared with the 63 Oe measured in the previous study. With this lower SAR value, LMFCPAS glass is considered to be a suitable material for a low-heat-generation device.

IV. Conclusions

The phase transformation and magnetic properties of $10Li_2O$-$9MnO_2$-$16Fe_2O_3$-$15CaO$-$5P_2O_5$-$5Al_2O_3$-$40SiO_2$ (LMFCPAS) glass have been studied using XRD, SEM, EDS, TEM and SAED. The $Li_2Al_2Si_3O_{10}$, β-$CaSiO_3$ and $FeFe_2O_4$ phases were formed when the LMFCPAS glass was crystallized at 750 °C for 2 h. With crystallization at 850 °C for 4 h, $Li_2Al_2Si_3O_{10}$, Li_2SiO_3, β-$CaSiO_3$, Li_3PO_4, $FeFe_2O_4$ and Li(Mn,Fe)PO_4 phases are found and identified in the LMFCPAS glass-ceramics. Both β-wollastonite and lithium silicate exhibited lath morphology and directional growth. The LMFCPAS glass crystallized at 850 °C for 16 h has very low remnant induction (0.013 emu/g) and coercive force (16 Oe) under an applied magnetic field of 1000 Oe, and shows the ferromagnetic behavior of an inverse spinal structure.

Acknowledgment

This work was supported by the National Science Council, Taiwan (Rep. of China) under Contract No. NSC-97 – 2211-E-239 – 001-MY, which is gratefully acknowledged. The authors thank Mr H.Y. Yao of National Cheng Kung University for providing TEM image assistance in the experimental work.

References

1 Ohura, K., Ikenaga, M., Nakamura, T., Yamamuro, T., Ebisawa, Y., Kokubo, T., Kotoura, Y., Oka, M.: A heat-generating bioactive glass-ceramic for hyperthermia, *J. Appl. Biomater.*, **2**, 153 – 159, (1991).

2 Leventouri, T., Kis, A.C., Thompson, J.R., Anderson, I.M.: Structure, microstructure and magnetism in ferromagnetic bioceramics, *Biomaterials*, **26**, 4924 – 4931, (2005).

3 Singh, R.K., Kothiyal, G.P., Srinivasan, A.: Magnetic and structural properties of CaO-SiO_2-P_2O_5-Na_2O-Fe_2O_3 glass ceramics, *J. Magn. Magn. Mater.*, **320**, 1352 – 1356, (2008).

4 Luderer, A.A., Borrelli, N.F., Panzarino, J.N., Mansfield, G.R., Hess, M., Brown, J.R., Barnet, E.H.: Glass-ceramic-mediated, magnetic-field-induced localized hyperthermia: response of a murine mannary carcinoma, *Radiat. Res.*, **94**, 190 – 198, (1983).

5 Oh, S.H., Choi, S.Y., Lee, Y.K., Kim, K.N.: Research on annihilation of cancer cells by glass-ceramics for cancer treatment with external magnetic field. I. preparation and toxicity, *J. Biomed. Mater. Res.*, **54**, 360 – 365, (2001).

6 Hsi, C.S., Wang, M.C.: Crystallization kinetics and phase transformation of Li_2O-Fe_2O_3-MnO_2-CaO-P_2O_5-SiO_2 glass, *J. Mater. Res.*, **13**, 2655 – 2661, (1998).

7 Wang, M.C., Wang, C.F., Hsi, C.S.: Crystallization kinetics and morphology of an Li_2O-MnO_2-Fe_2O_3-CaO-P_2O_5-SiO_2 glass, *Glastech.Ber. Glass Sci. Technol.*, **73C1**, 82 – 89, (2000).

8 Hsi, C.S., Cheng, H.Z., Hsu, H.J., Chen, Y.S., Wang, M.C.: Crystallization kinetics and magnetic properties of iron oxide contained $25Li_2O$-$8MnO_2$-$20CaO$-P_2O_5-$45SiO_2$ glasses, *J. Eur. Ceram. Soc.*, **27**, 3171 – 3176, (2007).

9 Ferreira da Sila, M.G., Costa, B.F.O.: The effect of composition and temperature on the amount and type of nanoferrite

particles inserted in Fe_2O_3-ZnO-MgO-SiO_2 glass-ceramics, *J. Non-cryst. Solids.*, **357**, 3722 – 3725, (2011).

10 Singh, R.K., Srinivasan, A.: Magnetic properties of bioactive glass-ceramics containing nanocrystalline zinc ferrite, *J. Magn. Magn. Mater.*, **323**, 330 – 333, (2011).

11 Mirkazemi, S.M., Marghussian, V.K., Beitollahi, A.: Microstructure and magnetic properties of BaO-Fe_2O_3-B_2O_3-SiO_2 glass ceramic, *Ceram. Int.*, **32**, 43 – 51, (2006).

12 Lee, C.K., Berta, R.F., Speyer, R.F.: Effect of Na_2O addition in the crystallization of barium ferrite from a BaO-B_2O_3-Fe_2O_3 glass, *J. Am. Ceram. Soc.*, **79**, 183 – 192, (1996).

13 Singh, R.K., Srinivasan, A.: Bioactivity of ferromagnetic MgO-CaO-SiO_2-P_2O_5-Fe_2O_3 glass-ceramics, *Ceram. Int.*, **32**, 283 – 290, (2010).

14 Mirkazemi, S.M., Marghussian, V.K., Beitollahi, A., Dou, S.X., Wexler, D., Konstaninov, K.: Effect of ZrO_2 nucleant on crystallization behavior, microstructure and magnetic properties of BaO-Fe_2O_3-B_2O_3-SiO_2 glass ceramics, *Ceram. Int.*, **33**, 463 – 469, (2007).

15 Chikazumi. S., Taketomi, S., Ukita, M., Mizukami, M., Miyajima, H., Setogawa, M., Kurihara, M.: Physics of magnetic fluids, *J. Magn. Magn. Mater.*, **65**, 245 – 251, (1987).

16 Wu, C.S., Hsi, C.S., Hsu, F.C., Wang, M.C., Chen, Y.S.: Magnetism and thermal induced characteristics of Fe_2O_3 content bioceramics, *J. Magn. Magn. Mater.*, **324**, 3918 – 3923, (2012).